

Characterization and Quantification of Particle-Bound Criegee Intermediates in Secondary Organic Aerosol

Steven J. Campbell,* Kate Wolfer, Peter J. Gallimore, Chiara Giorio, Daniel Häussinger, Marc-Aurèle Boillat, and Markus Kalberer



Cite This: *Environ. Sci. Technol.* 2022, 56, 12945–12954



Read Online

ACCESS |

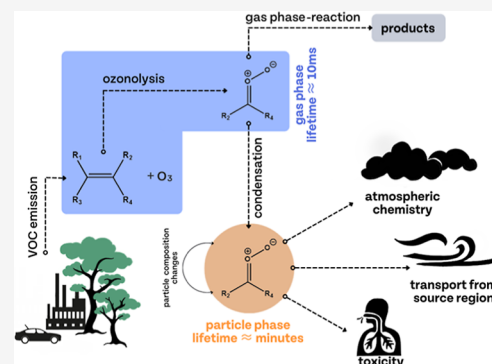
Metrics & More

Article Recommendations

Supporting Information

ABSTRACT: The ozonolysis of alkenes contributes substantially to the formation of secondary organic aerosol (SOA), which are important modulators of air quality and the Earth's climate. Criegee intermediates (CIs) are abundantly formed through this reaction. However, their contributions to aerosol particle chemistry remain highly uncertain. In this work, we present the first application of a novel methodology, using spin traps, which simultaneously quantifies CIs produced from the ozonolysis of volatile organic compounds in the gas and particle phases. Only the smallest CI with one carbon atom was detected in the gas phase of a β -caryophyllene ozonolysis reaction system. However, multiple particle-bound CIs were observed in β -caryophyllene SOA. The concentration of the most abundant CI isomer in the particle phase was estimated to constitute $\sim 0.013\%$ of the SOA mass under atmospherically relevant conditions. We also demonstrate that the lifetime of CIs in highly viscous SOA particles is at least on the order of minutes, substantially greater than their gas-phase lifetime. The confirmation of substantial concentrations of large CIs with elongated lifetimes in SOA raises new questions regarding their influence on the chemical evolution of viscous SOA particles, where CIs may be a previously underestimated source of reactive species.

KEYWORDS: secondary organic aerosol, Criegee Intermediates, mass spectrometry, spin traps, sesquiterpenes, ozonolysis



1. INTRODUCTION

The oxidation of biogenic and anthropogenic volatile organic compounds (VOCs) by hydroxyl radicals ($\bullet\text{OH}$), ozone (O_3), and nitrate radicals ($\bullet\text{NO}_3$) is a significant process in defining the reactivity and composition of the lower atmosphere. An important reaction in the troposphere is the ozonolysis of alkenes, which contributes substantially to local photochemical smog.¹ This reaction generates a plethora of oxidized organic compounds and leads to the formation of secondary organic aerosol (SOA). Biogenic VOCs (BVOCs) are emitted in large quantities into the atmosphere, with sesquiterpene ($\text{C}_{15}\text{H}_{24}$) emissions alone estimated to be $\sim 30 \text{ Tg yr}^{-1}$, contributing up to 3% of global BVOC emissions.² Inclusion of updated sesquiterpene emissions and SOA formation pathways in a recent modeling study (considering β -caryophyllene-derived SOA only) produced a 48% increase in the global biogenic SOA burden relative to previous estimates, highlighting the potentially important contribution of sesquiterpenes such as β -caryophyllene SOA to the global SOA budget.³

The reaction of alkenes with O_3 proceeds through a generally accepted mechanism via the cycloaddition of ozone across the alkene double bond to form a primary ozonide (POZ), which promptly decomposes to form a carbonyl compound and a Criegee intermediate (CI).⁴ The CI is initially produced in a vibrationally excited state due to the

exothermic decomposition of the POZ,⁵ which can either undergo unimolecular decomposition to form other products, including hydroxyl radicals ($\bullet\text{OH}$) through the “hydroperoxide channel”, or undergo collisional stabilization to form the stabilized CI (SCI), which participates in a range of gas-phase bimolecular reactions with other species including H_2O , SO_2 , O_3 , and NO_x .^{6–8} Recent studies have suggested that the simplest CIs (CI_{C1}) are predominantly zwitterionic in character; however, mixing of their ground electronic state with the first triplet excited state, which is biradical in character, may explain the CI reactivity in the troposphere.⁹

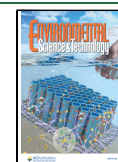
Additionally, the importance of highly oxygenated organic molecules (HOMs), species formed by an autooxidation mechanism involving peroxy radicals (RO_2) and intramolecular hydrogen-atom shifting, often irreversibly condensing into the particle phase,¹⁰ has recently become clear as they could constitute a critical link between particle nucleation and cloud condensation nuclei formation.^{10,11} It has been

Received: June 14, 2022

Revised: August 18, 2022

Accepted: August 22, 2022

Published: September 2, 2022



suggested that the ozonolysis of monoterpenes, proceeding through CI formation followed by the RO₂ autooxidation mechanism, can efficiently form HOMs.^{11,12} Scavenging of SCIs in the gas phase using organic bystander molecules, for example, formic acid, spin traps, and other organic compounds leads to a reduction in the concentrations of higher-molecular-weight compounds detected in SOA particles; this illustrates that gas-phase SCI reactions promote the formation of high-molecular-weight compounds, which efficiently partition to form SOA, thus influencing new particle formation.^{13–15} Reactive intermediates such as the CI or RO₂ are clearly of importance for the gas phase oxidation of VOCs. However, large uncertainty remains regarding the influence that particle-bound radicals and reactive intermediates have on SOA composition, aging, and potentially also health effects.^{16,17}

From an atmospheric perspective, the chemistry of condensed-phase CIs has been explored primarily by monitoring the products of CI reactions in the condensed phase, formed specifically by heterogeneous oxidation by O₃. Gallimore et al.³⁵ and Wang et al.¹⁸ demonstrated that the reaction of SCIs in oleic acid particles leads to the formation of high-molecular-weight compounds while providing mechanistic insight into the formation of various highly oxidized compounds in particle-phase reactions of CIs. Recently, Zhou et al.¹⁹ illustrated that acyloxyalkyl-1-hydroperoxides (AAHPs) are produced from the reaction of condensed-phase CIs with carboxylic acids by monitoring the decay of bystander molecules such as palmitic acid and heptanoic acid when squalene is exposed to ozone. Mochida et al.²⁰ also explored condensed-phase CI chemistry in methyl oleate aerosol and observed a range of high-molecular-weight products in the presence of myristic acid, including AAHPs. A range of recent studies have also shown that multiphase reactions of condensed-phase CIs can produce reactive oxygen species, such as H₂O₂²¹ and •OH, influencing the oxidative capacity and composition of the condensed phase, as well as producing a range of functionalized organic products.²² Arata et al. also demonstrated that the multiphase chemistry of CIs is relative humidity (RH)-dependent, where CI reactions with water have important consequences for gas-phase organic product distributions as well as influencing particle-phase composition.²³ These studies provide valuable mechanistic insight into the condensed-phase chemistry of CIs. However, further work is required to elucidate and especially quantify the role that both gas-phase CIs and particle-phase CIs play in the formation of highly oxidized components of SOA and their contribution to the absorption properties and health effects of aerosol particles.

Recently, we developed a novel method to characterize and quantify CIs in the gas phase by trapping CIs with spin-trap molecules.^{24,25} CIs generated from the ozonolysis of several atmospherically relevant VOCs were scavenged in the gas phase by the spin-trap 5,5-dimethyl-pyrroline-*N*-oxide (DMPO), forming a stable CI-DMPO adduct which is subsequently analyzed using proton-transfer reaction time-of-flight mass spectrometry (PTR-ToF-MS).^{24,25} This method is advantageous as it allows the quantification of CIs produced directly from the ozonolysis of alkenes, the process that forms CIs in the atmosphere, as opposed to CIs formed from diiodoalkane photolysis, a method which was used to form CIs in the gas phase in previous studies.^{26,27}

In this work, we expand our spin-trap methodology to unambiguously detect for the first time several CIs in SOA

particles formed from the ozonolysis of β -caryophyllene while simultaneously quantifying the CIs present in the gas phase. Using authentic synthesized CI-PBN standards, we estimate that the most abundant CI (CIC_{15k}, the C₁₅-CI with a terminal ketone group) alone constitutes about ~0.013% of the total SOA mass at near-ambient SOA mass concentrations of 136 $\mu\text{g}/\text{m}^3$. The lifetime of particle-bound CIs in SOA is at least on the order of minutes, much longer than the typical CI lifetime in the gas phase, highlighting the stabilization of CIs in highly viscous β -caryophyllene-derived SOA particles. This method enables the simultaneous characterization and quantification of CIs in the gas and particle phase, with the unique ability to quantify multiple reactive intermediates in complex multiphase reaction systems, providing new insights into the abundance and chemistry of CIs in both the gas and particle phases.

2. MATERIALS AND METHODS

2.1. Reagents. *trans*-(–)- β -Caryophyllene ($\geq 99\%$, Sigma-Aldrich) was reacted with ozone produced by a UV lamp (3SC-9 185/254 nm UV Appleton Woods). The spin-trap *N*-tert-butyl- α -phenylnitron (PBN) ($\geq 98\%$, GC grade, Sigma-Aldrich) was used to react with and stabilize CIs in the particle phase analysis. A more volatile spin-trap DMPO ($\geq 97\%$, GC grade, Sigma-Aldrich) was used to react with and stabilize CIs in the gas phase. Acetonitrile ($\geq 99.9\%$ Optima LC/MS grade, Fisher Chemical) was used as a solvent to facilitate CI capture in the particle-phase experiments using an impinger.

2.2. Flow Tube Setup for Gas-Phase CIs. CIs were produced from β -caryophyllene ozonolysis in a flow tube reactor maintained at ambient temperature (~ 23 °C) and pressure under dry conditions (relative humidity < 2%), which has been described in detail previously²⁴ and will be summarized in brief here. A schematic of the flow tube setup for the capture of both gas- and particle-phase CIs is presented in Figure S2. A flow of 0.2 L/min N₂ (oxygen-free nitrogen, BOC) carrier gas regulated via a 20–2000 cm³/min mass flow controller (MKS 1179A Mass-Flo controller) was passed over 1 mL of β -caryophyllene in a 50 mL round-bottom flask and heated to 60 °C using a water bath to introduce the gaseous organic precursor into the flow tube, producing a steady-state concentration of 25 ppm. Ozone was produced by flowing synthetic air (Zero grade, BOC) at 2 L/min through a glass tube containing a UV lamp (3SC-9 184/254 nm UV Appleton Woods). CIs in the gas phase were quantified by stabilization with spin-trap DMPO, with online detection of CI-DMPO adducts using a proton-transfer time-of-flight mass spectrometer (PTR-TOF 8000, Ionikon Analytik, Innsbruck, Austria) as extensively described previously.^{24,25} For the gas-phase setup, the total reaction time was approximately 3 s, which was previously optimized. A N₂ (oxygen-free nitrogen, BOC) carrier gas regulated via a 20–2000 cm³/min mass flow controller (MKS 1179A Mass-Flo controller) was passed through a pear-shaped flask containing 0.5 mL of DMPO and heated to 40 °C in a water bath at a flow rate of 0.2 L/min in order to evaporate DMPO into the gas phase and scavenge gas-phase CIs. The N₂ flow containing DMPO was then mixed with the sample flow from the flow tube using a T-fitting (Swagelok). DMPO was produced with an excess concentration of ~150 ppm to ensure efficient scavenging of gas-phase CIs.^{24,25} DMPO reacts with the CIs in a 1/4 inch poly(tetrafluoroethylene) tube heated at 80 °C before

quantification of the resulting CI-DMPO adducts using PTR-ToF-MS according to the procedure described in Section S1.9.

2.3. Flow Tube Setup for Particle-Phase CIs. For analysis of particle-phase CIs, the total residence time in the flow tube was approximately 67 s. SOA mass concentrations produced from the flow tube were measured using a TSI scanning mobility particle sizer composed of a TSI 3080 electrostatic classifier (X-ray neutralizer and differential classifier (X-ray neutralizer and differential classifier (TSI model 3081) and a condensation particle counter (TSI model 3775). The SOA flow was then passed through an activated charcoal denuder to remove any O_3 and VOCs, including gas-phase CIs, prior to SOA sampling. The average SOA mass concentrations generated in the flow tube for this set of experiments were between 51 and 476 $\mu\text{g m}^{-3}$ (Table S1), with a particle diameter mode between ~ 25 and 50 nm. Different SOA mass concentrations were produced by altering the O_3 concentration introduced into the flow tube between 26 and 470 ppb while keeping the β -caryophyllene gas-phase concentration constant at 2.2 ppm (Table S1). The particle-phase CIs were captured in a 50 mL impinger containing 10 mL of a 2 mM solution of PBN in acetonitrile. The impinger was submerged in an acetonitrile/dry ice bath maintained at approximately -41°C in order to improve the CI-PBN adduct stability in solution, as well as to limit solvent evaporation during sampling. The impinger was packed with glass beads in order to improve the SOA particle collection efficiency of the impinger.²⁸ The SOA was sampled for 2 h continuously before analysis in order to preconcentrate the CI-PBN adducts in the impinger before being analyzed using ultrahigh-performance liquid chromatography high-resolution mass spectrometry (UHPLC-HRMS) and nuclear magnetic resonance (NMR) spectroscopy, details of which can be found in Sections S1.2 and S1.7, respectively.

3. RESULTS AND DISCUSSION

3.1. Mechanism of Formation of Detected CIs. β -Caryophyllene reacts with O_3 in the gas phase to produce four first-generation CIs through the decomposition of both endocyclic and exocyclic POZs (Figure 1, red structures). The CI_{C15a} and CI_{C15k} are formed in the reaction of O_3 across the endocyclic double bond of β -caryophyllene, with *a* and *k* referring to the CI with a terminal aldehyde or a terminal ketone, respectively. The CI_{C1} and CI_{C14} are formed in the reaction of O_3 across the exocyclic double bond of β -caryophyllene, depending on the fragmentation of the POZ. Under the relatively dry conditions in this experimental setup, the two dominant stable first-generation products are β -caryophyllene aldehyde and the endocyclic β -caryophyllene secondary ozonide, which account for approximately 80% of the first-generation products formed from β -caryophyllene ozonolysis.²⁹ Both products retain one unsaturated C=C double bond, which can undergo further reaction with O_3 to produce second-generation CIs. A simplified reaction scheme showing the formation of first-generation CIs detected in this study and some further reactions leading to second-generation CIs is presented in Figure 1.

3.2. Quantification of CI-DMPO Adducts in the Gas Phase. Of the four possible first-generation CIs listed in Figure 1 (red structures) produced using the experimental setup described in Figure S2, only the CI_{C1} -DMPO adduct, with elemental formula $(C_7H_{13}NO_3)^+H^+$ (m/z 178.047), was detected in the gas phase with PTR-ToF-MS (Figure S5). The CI-DMPO adducts corresponding to the other first-generation

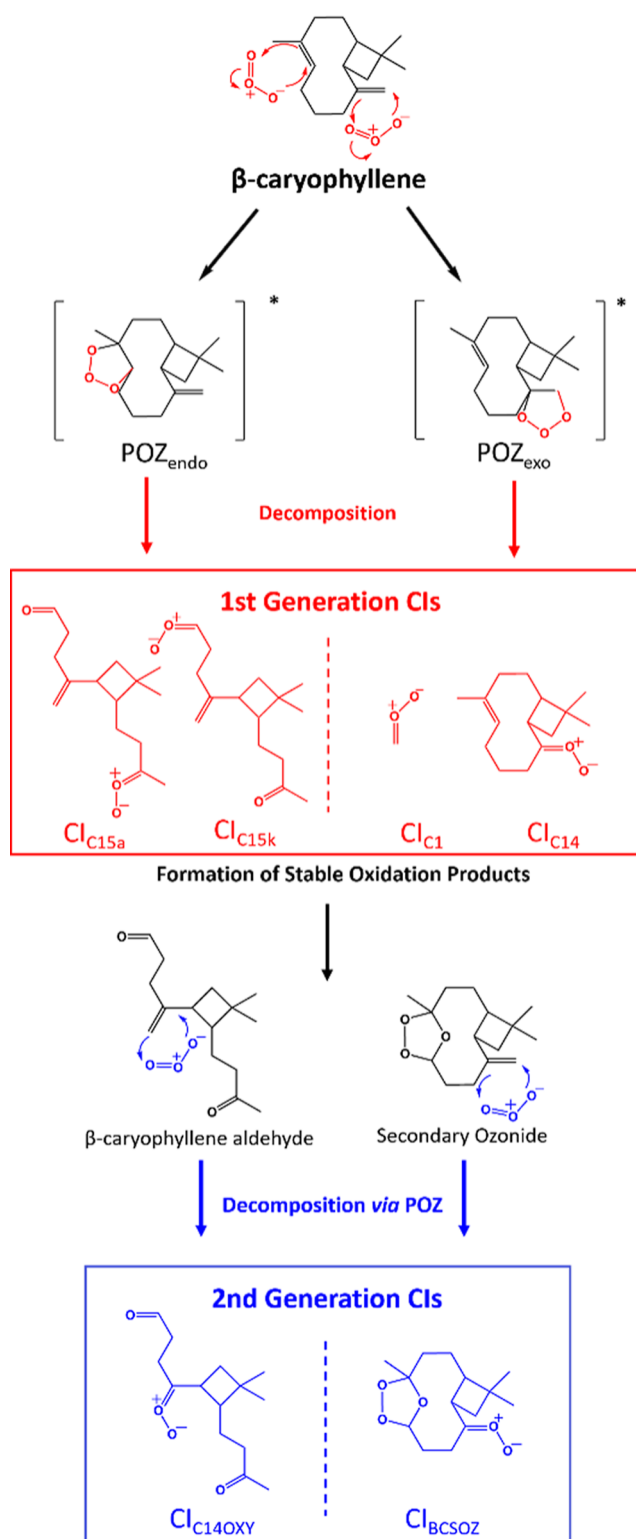


Figure 1. Simplified reaction scheme illustrating the formation pathways of CIs detected in this work. The precursor β -caryophyllene reacts with O_3 either via the endo- or exo-unsaturated C=C bond to produce four first-generation CIs (red structures). These CIs can produce stable oxidation products that can then undergo further reaction with O_3 . Two second-generation CIs (blue structures) were also detected, generated from secondary ozonolysis of stable oxidation products produced from β -caryophyllene ozonolysis.

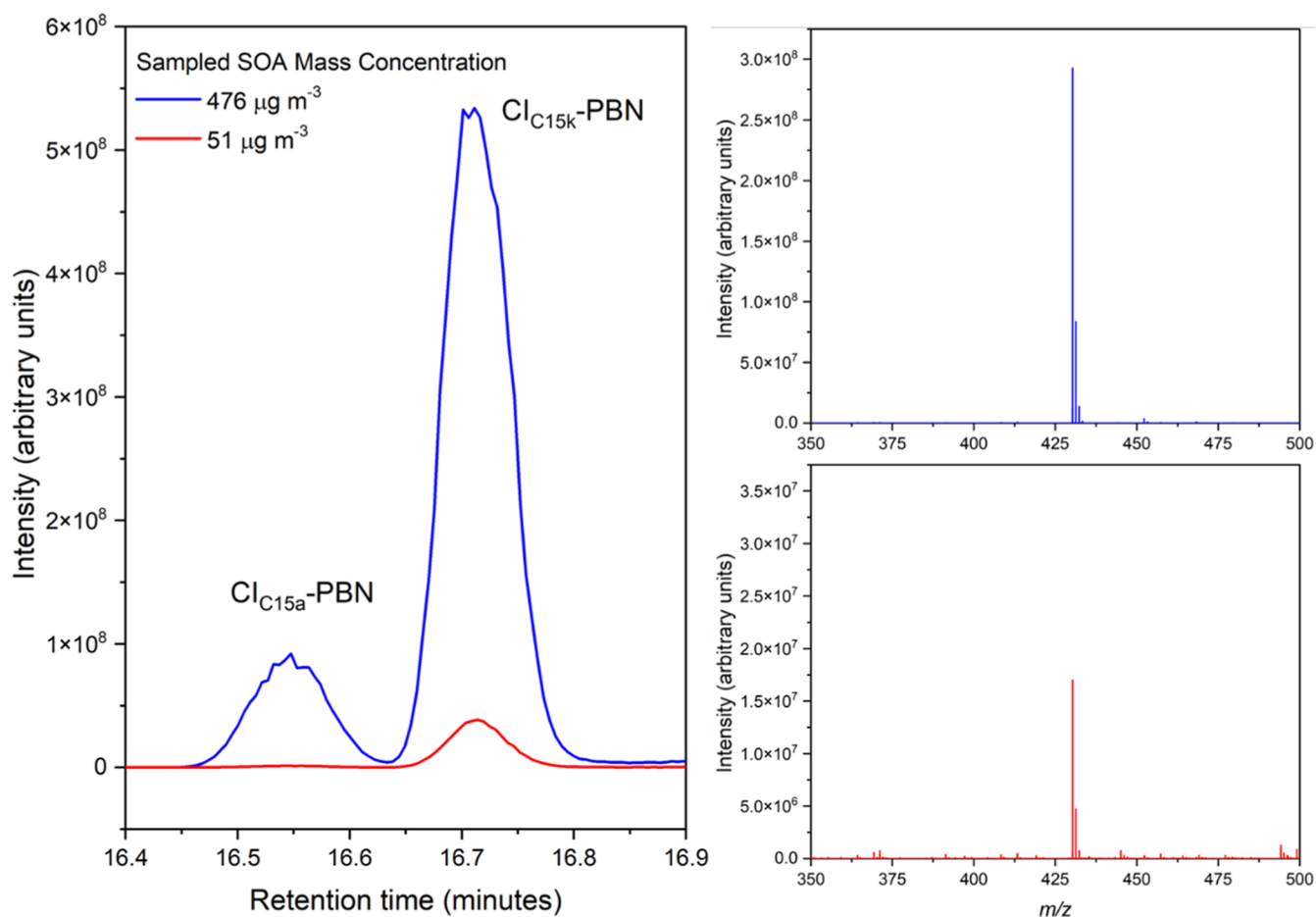


Figure 2. Extracted ion chromatograms of $\text{Cl}_{\text{C15a}}\text{-PBN}$ and $\text{Cl}_{\text{C15k}}\text{-PBN}$ (m/z 430.2951, $[\text{M} - \text{H}]^+$ adducts, retention times 16.54 and 16.72 min, respectively); the blue trace represents the particles sampled at a SOA mass concentration of $476 \mu\text{g m}^{-3}$, and the red trace represents CIs detected at $51 \mu\text{g m}^{-3}$. Panels to the right: mass spectra of the peak at 16.72 min for the $476 \mu\text{g m}^{-3}$ experiment (upper-right panel) and the $51 \mu\text{g m}^{-3}$ experiment (lower right panel). The first adduct corresponds to the $\text{Cl}_{\text{C14oxy}}$ which forms after the attack of O_3 across the exocyclic double bond of β -caryophyllene aldehyde, the second most abundant first-generation oxidation product (Figure 1, blue structures).

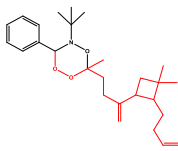
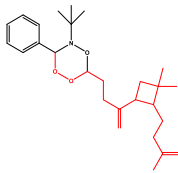
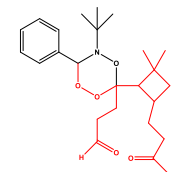
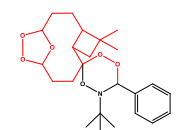
CIs (Cl_{C14} , Cl_{C15a} , and Cl_{C15k}) or any second-generation CIs (Figure 1, blue box) were not detected in the gas phase. For initial O_3 and β -caryophyllene concentrations of 25 and 21 ppm, respectively, $\text{Cl}_{\text{C1}}\text{-DMPO}$ steady-state concentrations of 13.7 ± 0.7 ppb (over three experimental repeats) were observed for a reaction time of 3 s. High precursor concentrations in the parts-per-million range, which were previously optimized,²⁵ are required specifically for gas-phase detection of the Cl_{C1} . The $\text{Cl}_{\text{C1}}\text{-DMPO}$ concentrations observed here are about 3 orders of magnitude lower than the initial concentration of the reactants.

Calculations using the Master Chemical Mechanism (MCM) v3.2²⁹ estimate a gas-phase mixing ratio of approximately 0.3 ppm for the Cl_{C1} 3 s after the start of the gas-phase reaction, approximately 1 order of magnitude greater than detected in our study. This modeled concentration is likely an upper limit for the Cl_{C1} as the MCM mechanism neglects $\text{Cl} + \text{Cl}$, $\text{Cl} + \text{O}_3$, and $\text{Cl} + \text{organic}$ reactions.²⁹ The data shown here is consistent with our previous results,²⁰ in which the $\text{Cl}_{\text{C1}}\text{-DMPO}$ adduct had the largest observed concentration for a variety of alkene precursors where there were more than one CIs formed from the initial ozonolysis. Density functional theory (DFT) calculations in our previous study suggested that the Cl_{C1} reaction with DMPO proceeds through a barrierless pathway, probably contributing to more

efficient scavenging of the Cl_{C1} by DMPO relative to that of larger CIs.²⁰ The large first-generation CIs (Cl_{C14} , Cl_{C15a} , and Cl_{C15k}) were not detected in the gas phase. This could be partially due to their enhanced unimolecular decay rate constants compared to the Cl_{C1} ; theoretical calculations show that larger CIs, such as Cl_{C10} and Cl_{C9} derived from α -pinene (*E*-pinonaldehyde-*K*-oxide 2 s^{-1} , *Z*-pinonaldehyde-*K*-oxide 60 s^{-1}) and β -pinene (*Z*-nopinone-oxide 250 s^{-1}), have greater unimolecular decay rates compared to Cl_{C1} (0.3 s^{-1}).³⁰ However, given their larger size and thus reduced volatility, larger CIs produced in this ozonolysis regime could be of sufficiently low volatility that they partition into the particle phase and hence would elude detection in the gas phase.

3.3. Identification of Particle-Bound CIs in SOA. To confirm the presence of larger, lower-volatility CIs produced from β -caryophyllene ozonolysis in the particle phase, SOA particles were scavenged in an impinger containing the spin-trap PBN in acetonitrile. The same flow tube setup illustrated in Figure S2 was used, but with much lower gas-phase precursor concentrations compared to the gas-phase experiments described previously, resulting in SOA particle mass concentrations of $51\text{--}476 \mu\text{g m}^{-3}$ (Table S1). After 2 h of SOA sampling, followed by sample preconcentration and subsequent UHPLC-HRMS analysis (Section S1.2), two peaks were detected and assigned to the adduct formed between

Table 1. Summary of Annotated CI-PBN Adducts Assigned in This Study

CI-PBN Adduct [M+H] ⁺	Neutral Molecular formula	Measured mass (Da)	Mass error (ppm)	Number of peaks	Retention time (mins)	Proposed Structure ^[a]
CI _{C15a} -PBN	C ₂₆ H ₃₉ O ₄ N	430.2951	-0.20	1	16.54	
CI _{C15k} -PBN	C ₂₆ H ₃₉ O ₄ N	430.2951	-0.20	1	16.72	
CI _{C14oxy} -PBN	C ₂₅ H ₃₇ O ₅ N	432.2743	-0.35	1	13.73	
CI _{BCSOZ} -PBN and isomers	C ₂₅ H ₃₇ O ₆ N	448.2695	0.30	2	17.07 17.20	

^aStructures based on previous studies^{24,25} and NMR characterization of the CI_{C15}-PBN, assuming analogous reactivity of other CIs with PBN. Black structure is the spin trap PBN, red structure is the CI.

spin-trap PBN and the CI_{C15a} and CI_{C15k} isomers, respectively (Figure 2).

Proposed structures of all CI-PBN adducts detected in this study using UHPLC-HRMS are presented in Table 1. The difference between the two measured peak areas of the CI_{C15a}-PBN and CI_{C15k}-PBN shown in Figure 2 is likely due to the increased stability of the CI_{C15k}-PBN adducts compared to CI_{C15a}-PBN, analogous to our earlier results.²⁴ No first-generation CI_{C14}-PBN or CI_{C1}-PBN adducts were detected in the SOA particles. This is likely due to the relatively high volatility of the CI_{C1}, which would therefore not partition into the particle phase, as well as to the lower yield of CI_{C1} and CI_{C14} compared to CI_{C15a} and CI_{C15k}. Given that the endocyclic double bond is 20–100 times more reactive toward ozone compared with the exocyclic double bond, this increased reactivity promotes the formation of the CI_{C15k} and CI_{C15a} via endocyclic ozonolysis.^{31,32} In addition, a series of second-generation CIs can form, produced from secondary ozonolysis of the remaining unsaturated C=C bond present in stable first-generation organic products. We detected two additional second-generation CI-PBN adducts at *m/z* 448.2695 ((C₂₅H₃₇NO₆)H⁺) and *m/z* 432.2743 ((C₂₅H₃₇NO₅)H⁺) (Table 1).

Furthermore, an additional second-generation CI adduct has been tentatively assigned to the CI_{BCSOZ} (Figure 1, Table 1), formed after the attack of O₃ across the remaining exocyclic bond on the secondary ozonide. Under the dry experimental conditions ([H₂O] < 2 ppm) used here, calculations using the MCM predict the β -caryophyllene secondary ozonide to be the dominant first-generation oxidation product, with an estimated yield \geq 65%, due to the tendency of the CI to undergo ring closure under dry conditions.²⁹ Proposed structures of the four particle-phase CI-PBN adducts detected are reported in Table

1, postulated on the basis of the reaction scheme for β -caryophyllene ozonolysis,²⁹ NMR structural identification, exact mass measurements using UHPLC-ESI-HRMS, and in analogy to the comprehensive analysis of CI-PBN adducts in our previous studies using HPLC-HRMS, MS/MS, DFT calculations, and NMR spectroscopy.^{24,25} For the present study, we synthesized authentic CI_{C15k}-PBN adduct standards produced by bulk ozonolysis, which were then isolated using UHPLC separation and used for UHPLC-HRMS quantification standards (Sections S1.2–S1.4) and NMR structural confirmation of the CI-PBN structures. The synthesized and isolated CI_{C15k}-PBN adduct was analyzed by two-dimensional NMR experiments (Figures S13–S19), which allowed the unambiguous confirmation of the postulated structure for the CI_{C15k}-PBN adduct. Detailed NMR analysis can be found in Section S2.7.

The detection of CI_{C15a}-PBN and CI_{C15k}-PBN, CI_{BCSOZ}-PBN, and CI_{C14oxy}-PBN adducts using the PBN spin trap in this experimental setup demonstrates that CIs generated from both primary and secondary ozonolysis can persist in the particle phase for a time on the order of minutes. This is due to the residence time of the particles in the experimental system prior to collection (67 s); gas-phase chemistry should reach completion in seconds (according to MCM calculations), and any potential gas phase artifacts (including O₃) are efficiently removed by an activated charcoal denuder; thus, the particle-phase CIs must persist on the order of minutes to be scavenged in the impinger containing the PBN spin trap. It is not possible with the current data to fully determine whether the first and second-generation particle-bound CIs detected here are the result of either gas-phase formation of low-volatile CIs with subsequent rapid partitioning into the SOA particles or formed through the heterogeneous reaction of O₃ with precursors

already present in the particles. Nonetheless, these results highlight that particle-phase reactive intermediates and radicals, which are of key importance in atmospheric chemistry, can be selectively scavenged in situ and stabilized for detailed offline quantitative analysis using this methodology. A range of additional stable, nonradical SOA oxidation products formed from β -caryophyllene ozonolysis were also identified in the UHPLC-HRMS analysis and are presented in Table S4, which compare well with previous literature findings, demonstrating that the SOA formed in our experiments was very similar in composition to previous β -caryophyllene-SOA studies.

These chromatography, mass spectrometry, and NMR results represent the first simultaneous, unambiguous detection of gas-phase and particle-bound CIs in an ozonolysis multiphase reaction system. In summary, we detected and identified four of the most abundant CIs in the particle phase that are expected to be formed under the experimental conditions used here, that is, the CI_{C15a} and CI_{C15k} which are the most abundant first-generation CIs and two of the most abundantly formed second-generation CIs ($\text{CI}_{\text{C14oxy}}$, CI_{BCSOZ}). This demonstrates that the experimental and unique analytical strategy developed here can capture the diversity of CIs formed in the complex multiphase oxidation schemes of atmospherically important alkenes.

3.4. Quantification of CI_{C15k} in the Particle Phase. To quantify the CI_{C15k} -PBN adduct, a CI_{C15k} -PBN standard was synthesized using the bulk ozonolysis method described in Section S1.1 in the Supporting Information. The CI_{C15k} isomer was chosen for both quantification purposes and NMR structural elucidation as it has a more intense peak in the UHPLC-ESI-HRMS chromatogram than any other detected CI-PBN adduct (Figure 2). The UHPLC-ESI-HRMS peak area response as a function of CI_{C15k} -PBN concentration was then used as a calibration curve (Figure S12).

The CI_{C15k} -PBN adduct had the highest observed concentrations, normalized for SOA mass at the highest SOA mass concentrations sampled in this study, as shown in Figure 2; the calculated concentration of CI_{C15k} accounts for the collection efficiency of the impinger with respect to SOA mass (see Section S1.9) and for the estimated 24% trapping efficiency of PBN toward the CI_{C15k} (see Section S1.10). The concentration of CI_{C15k} -PBN detected here ranges from 2.1 ± 0.7 – 35.1 ± 3 pmol μg^{-1} , mass-normalized using the SOA mass concentrations ranging from 130–476 $\mu\text{g m}^{-3}$, respectively. The CI_{C15k} alone contributes between ~ 0.013 and 0.23% of the total SOA mass at a SOA concentration range of 130–476 $\mu\text{g m}^{-3}$ at the time of scavenging, approximately 67 s after the β -caryophyllene + O_3 is mixed in the gas phase.

3.5. Discussion. By utilizing our novel spin-trap methodology which can simultaneously scavenge and stabilize CIs in both the gas and particle phases, this study confirms the presence of large CIs (C_{14} – C_{15}) in SOA particles. We identify for the first-time secondary CIs produced from the ozonolysis of primary oxidation products (e.g., β -caryophyllene aldehyde), which persist in the particle phase and were not detected in the gas phase. Furthermore, we demonstrate the surprisingly long lifetime of particle-bound CIs in viscous β -caryophyllene SOA particles, which in this experimental regime is at least on the order of minutes and orders of magnitude greater compared to their gas-phase lifetime which is typically on the order of milliseconds.

The gas-phase lifetimes ($\tau_{\text{gas}} = 1/k_{\text{gas}}$) of these large CIs are short, so their detection in aerosols here after more than 1 min reaction time is interesting. It suggests that a fraction condenses onto the growing SOA and is preserved there, at least for the length of the experiment and potentially on much longer timescales. We show here that this is consistent with the known properties of β -caryophyllene CIs and SOA in our experimental conditions. For the CI_{C15k} quantified in Figure 3,

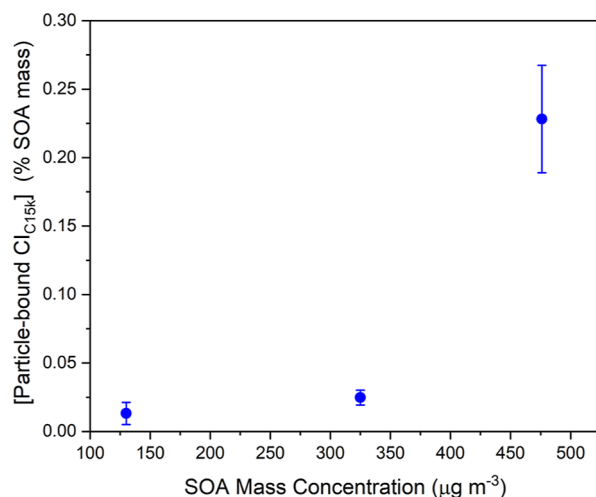


Figure 3. Measured CI_{C15k} concentrations, expressed as a percentage of the SOA mass. Error bars for measured values represent the standard deviation of the UHPLC-HRMS peak area observed over three experimental repeats.

an upper limit to τ_{gas} (of 12 ms) is provided by the unimolecular reaction of CIs to form the secondary ozonide.²⁹ Bimolecular reactions involving water, which are an important CI sink in the atmosphere, will be less significant under the dry conditions in our experimental setup, but reactions with abundant organic vapors generated during oxidation, or ozone itself, may reduce τ_{gas} further.³³

Given that all β -caryophyllene reacts within a few seconds (according to MCM calculations), and O_3 and gas-phase VOCs are efficiently removed by an activated charcoal denuder (Figure S1.2), no new CI_{C15k} should be produced in the gas phase. Therefore, the CIs detected in the impinger must reside in the particle phase to persist for the ~ 67 s residence time in the flow setup (Figure S1.2) prior to collection and trapping by PBN in the impinger. The particle-phase kinetics of CIs are not known, but the lifetimes of C_9 CIs in liquid SOA were inferred to be ~ 1 s at most.³⁴ However, β -caryophyllene SOA is highly viscous under dry conditions, with a diffusion coefficient $\sim 10^{-18}$ $\text{m}^2 \text{s}^{-1}$ corresponding to a ~ 1 h mixing timescale for a 200 nm particle.³⁵ CI uptake to such particles would efficiently preserve them, reducing further reaction in the aerosol phase or repartitioning back to the gas phase where they would be lost.

Assuming that uptake to particles is irreversible, and further CI reaction is efficiently inhibited, only a small conversion of gas-phase CIs to particles is required to explain the yields shown in Figure 3 (approx. 0.01–0.20%). This fraction converted to SOA can be expressed as $k_{\text{het}}/k_{\text{gas}}$, where k_{het} is the condensation sink to SOA and would need to be on the order of 10^{-2} to 10^{-1} s^{-1} , given that $k_{\text{gas}} \geq 10^2$ s^{-1} . Accommodation coefficients for organic species interacting with SOA are thought to be close to unity,³⁶ and the surface

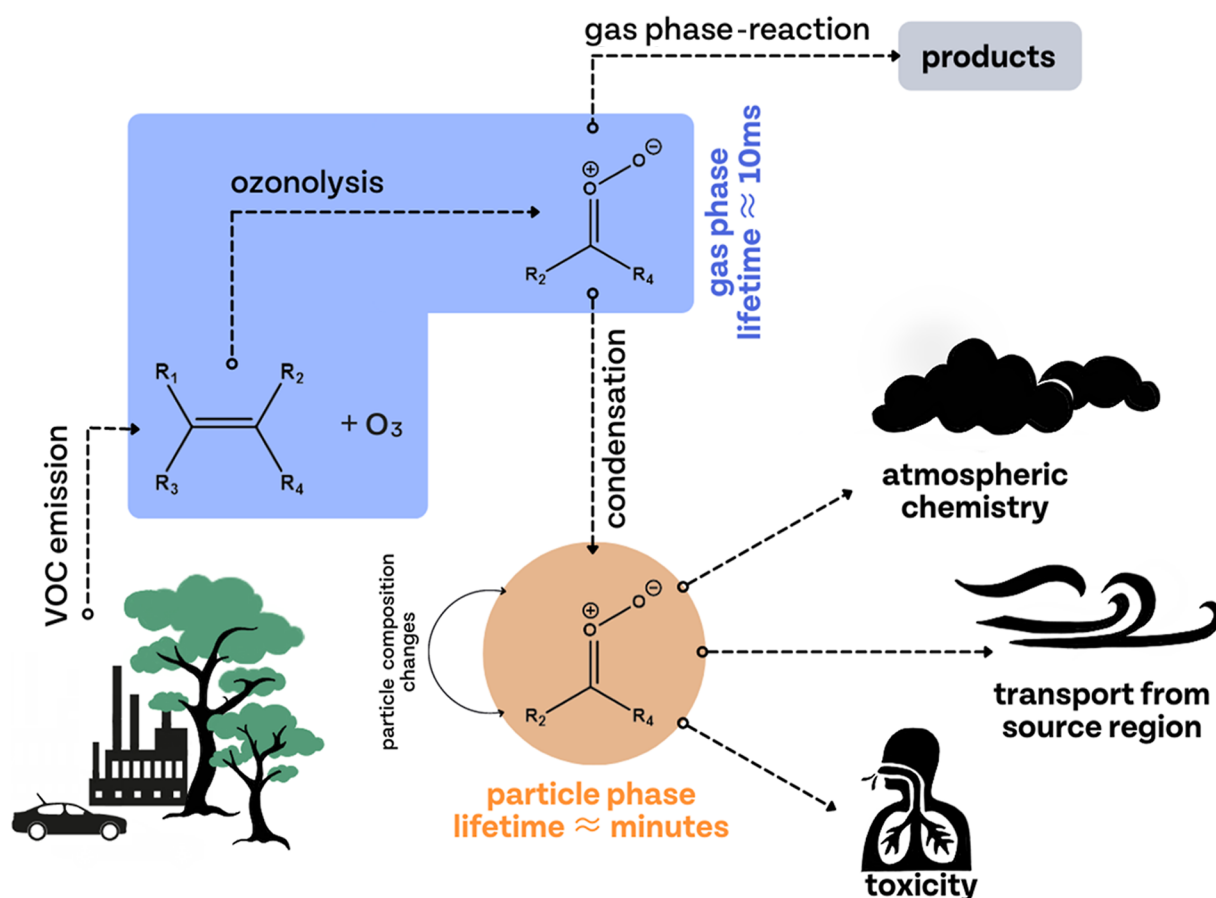


Figure 4. Simplified schematic representation of the potential fate of CIs formed from the gas-phase ozonolysis of VOC precursors. Sufficiently low-volatility CIs can partake in gas-phase chemistry and may also partition into the condensed phase, where their lifetime is elongated in viscous SOA. This likely results in changes to SOA composition, in turn influencing particle impacts on atmospheric chemistry and health. The greater stability of particle-bound CIs in SOA particles may facilitate the transport of these typically reactive species away from their emission source.

area densities measured are relatively high ($\sim 10^{-4}$ cm²/cm³)—hence, such uptake rates seem highly plausible and an illustrative calculation in the [Supporting Information](#) (Section S2.6) results in $k_{\text{het}} \sim 10^{-1}$ s⁻¹ for these conditions. While this estimate is simplified, it supports the hypothesis that CIs are formed in the gas phase and efficiently preserved in a viscous aerosol matrix. Furthermore, it suggests that even at ambient aerosol concentrations, such uptake may be an important source of particle-phase reactive intermediates and radicals.

This rapid partitioning and subsequent stabilization of large β -caryophyllene derived CIs in viscous SOA particles may have important consequences on the influence of CI chemistry on SOA particle composition, for example, by promoting the enhanced formation of α -acyloxyalkyl hydroperoxides in the condensed phase through the reaction of particulate-stabilized CIs with organic acids, or indeed H₂O to form α -hydroxyalkyl hydroperoxides, as opposed to, for example, secondary ozonide or β -caryophyllene aldehyde formation, which are the dominant reaction products in the gas phase,²⁹ thus potentially influencing SOA composition. In addition, studies investigating the heterogeneous oxidation of alkenes and subsequent multiphase CI chemistry have demonstrated that interactions of condensed-phase CIs with water vapor can lead to the formation of H₂O₂,²¹ as well as free radicals and reactive oxygen species,³⁷ with changes in relative humidity altering multiphase CI chemistry and having an impact on gas-phase product distributions as well as particle-phase composition.²³

We observed no obvious degradation of the CI_{C15}-PBN adduct over 48 h in UHPLC-HRMS analyses and more than 20 h in NMR analysis when temperatures were controlled at 4 or 10 °C, respectively ([Figures S6 and S14](#)). Therefore, in principle, this method could be applied to scavenge CIs in ambient studies where longer sampling times would be required due to the much lower ambient sample concentrations, facilitating the detection of particle-bound CIs in ambient aerosol particle samples. This method also has the potential to be adapted to scavenge other radical species in particles, including organic peroxy radicals (RO₂).³⁸ Typical estimated RO₂ radical lifetimes are on the order of 0.5 s (polluted, high NO) to 100 s (pristine, low NO); therefore, their lifetime in the ambient is comparable with (if not greater than) that of gas-phase CIs.¹⁰ Thus, it is feasible that low-volatility RO₂ radicals could also partition into the particle phase in competition with gas-phase losses, as evidenced in this study for CIs. This highlights the applicability of this methodology in future studies to simultaneously quantify gas-phase and particle-phase RO₂ radicals.

Using authentic synthesized CI_{C15k}-PBN standards, we estimate the concentrations of the CI_{C15k} to be between 2.1 ± 0.7 – 35.1 ± 3 pmol μg^{-1} , equivalent to 0.013–0.23% of the total SOA mass at corresponding SOA mass concentrations of 130–476 $\mu\text{g m}^{-3}$, respectively. To our knowledge, this is the first assessment of the concentration of particle-bound CIs formed from gas-phase ozonolysis, which are unambiguously

characterized using the spin-trap methodology in conjunction with NMR analysis. At the lowest value of $2.1 \pm 0.7 \text{ pmol } \mu\text{g}^{-1}$, close to atmospherically relevant biogenic SOA concentrations ($130 \text{ } \mu\text{g m}^{-3}$), the mass-normalized concentration of CI_{C15k} is comparable to other radicals and reactive intermediates measured in previous studies; for instance, Tong et al.³⁹ estimated that radical yields from HOM decomposition were between $1.8 \text{ pmol } \mu\text{g}^{-1}$ (naphthalene SOA) to $5.8 \text{ pmol } \mu\text{g}^{-1}$ (β -pinene SOA). Thus, the CI_{C15k} quantified here is on the same order of magnitude as these radical species and could constitute another important and previously unknown type of particle-bound reactive intermediate which contributes to the overall oxidative properties of SOA, either directly or through the formation of high molecular-weight oxidized products in SOA particles. In addition, our previous study using a profluorescent nitroxide spin trap estimated the total concentration of particle-bound organic radicals in β -caryophyllene SOA to be $2.5 \pm 0.7 \text{ pmol } \mu\text{g}^{-1}$, again on the same order of magnitude as CI_{C15k} measured in this study.¹⁵ As summarized in Figure 4, condensation of low-volatility CIs into the particle phase could represent a previously unknown source of reactive intermediates in the particle phase, altering SOA composition and preserving relatively high concentrations of longer-lived CIs under high-viscosity conditions; this could have important consequences in terms of SOA composition, which in turn influences the health effects of particles upon inhalation, as well as the atmospheric chemistry of SOA. This study demonstrates both the long lifetime of particle-bound CIs present in β -caryophyllene SOA, as well as their relatively high concentrations, which are comparable to concentrations of other types of particle-bound radicals in a range of SOA systems, opening up new questions regarding the role that CIs play in the chemical evolution of SOA particles in the atmosphere.

■ ASSOCIATED CONTENT

SI Supporting Information

The Supporting Information is available free of charge at <https://pubs.acs.org/doi/10.1021/acs.est.2c04101>.

Methods used, gas-phase ozonolysis results, UHPLC analysis on the stability of CI-PBN adducts, tandem MS assignment, negative electrospray ionization products, additional quantification data related to Section 3.2, calculations related to heterogeneous uptake of CIs versus gas-phase loss, and additional NMR data for CI-PBN structural characterization (PDF)

■ AUTHOR INFORMATION

Corresponding Author

Steven J. Campbell – Department of Environmental Sciences, University of Basel, Basel 4056, Switzerland; Yusuf Hamied Department of Chemistry, University of Cambridge, Cambridge CB2 1EW, U.K.; orcid.org/0000-0002-1334-3681; Email: stevenjohn.campbell@unibas.ch

Authors

Kate Wolfer – Department of Environmental Sciences, University of Basel, Basel 4056, Switzerland
Peter J. Gallimore – Department of Earth and Environmental Sciences, University of Manchester, Manchester M13 9PS, United Kingdom

Chiara Giorio – Yusuf Hamied Department of Chemistry, University of Cambridge, Cambridge CB2 1EW, U.K.; orcid.org/0000-0001-7821-7398

Daniel Häussinger – Department of Chemistry, University of Basel, Basel 4056, Switzerland; orcid.org/0000-0002-4798-0072

Marc-Aurèle Boillat – Department of Chemistry, University of Basel, Basel 4056, Switzerland

Markus Kalberer – Department of Environmental Sciences, University of Basel, Basel 4056, Switzerland

Complete contact information is available at: <https://pubs.acs.org/10.1021/acs.est.2c04101>

Author Contributions

S.J.C., C.G., and M.K. designed the research; S.J.C., K.W., C.G., and P.J.G. performed the research. D.H. and M.A.B. performed NMR analysis. S.J.C., K.W., P.J.G., C.G., and D.H. analyzed the data. All authors contributed to writing and editing the manuscript.

Funding

This work was funded by the European Research Council (ERC grant 279405) and Natural Environment Research Council (NERC) (NE/K008218/1). This work has also received funding from the European Union's Horizon 2020 Research and Innovation Programme through the EURO-CHAMP-2020 Infrastructure Activity under grant agreement no. 730997 and the Swiss National Science Foundation (200021_192192/1).

Notes

The authors declare no competing financial interest.

■ REFERENCES

- (1) Vereecken, L.; Harder, H.; Novelli, A. The reaction of Criegee intermediates with NO, RO₂, and SO₂, and their fate in the atmosphere. *Phys. Chem. Chem. Phys.* **2012**, *14*, 14682–14695.
- (2) Guenther, A. B.; Jiang, X.; Heald, C. L.; Sakulyanontvittaya, T.; Duhl, T.; Emmons, L. K.; Wang, X. The Model of Emissions of Gases and Aerosols from Nature Version 2.1 (MEGAN2.1): An Extended and Updated Framework for Modeling Biogenic Emissions. *Geosci. Model Dev.* **2012**, *5*, 1471–1492.
- (3) Khan, M. A. H.; Jenkin, M. E.; Foulds, A.; Derwent, R. G.; Percival, C. J.; Shallcross, D. E. A Modeling Study of Secondary Organic Aerosol Formation from Sesquiterpenes Using the STOCHEM Global Chemistry and Transport Model. *J. Geophys. Res.* **2017**, *122*, 4426–4439.
- (4) Criegee, R. Mechanism of Ozonolysis. *Angew. Chem., Int. Ed. Engl.* **1975**, *14*, 745–752.
- (5) Chhantyal-Pun, R.; Khan, M. A. H.; Taatjes, C. A.; Percival, C. J.; Orr-Ewing, A. J.; Shallcross, D. E. Criegee Intermediates: Production, Detection and Reactivity. *Int. Rev. Phys. Chem.* **2020**, *39*, 385–424.
- (6) Vereecken, L. Chemistry. Lifting the veil on an old mystery. *Science* **2013**, *340*, 154–155.
- (7) Welz, O.; Eskola, A. J.; Sheps, L.; Rotavera, B.; Savee, J. D.; Scheer, A. M.; Osborn, D. L.; Lowe, D.; Murray Booth, A.; Xiao, P.; Khan, M. A. H.; Percival, C. J.; Shallcross, D. E.; Taatjes, C. A. Rate Coefficients of C1 and C2 Criegee Intermediate Reactions with Formic and Acetic Acid near the Collision Limit: Direct Kinetics Measurements and Atmospheric Implications. *Angew. Chem., Int. Ed.* **2014**, *53*, 4547–4550.
- (8) Kalinowski, J.; Heinonen, P.; Kilpeläinen, I.; Räsänen, M.; Gerber, R. B. Stability of Criegee Intermediates Formed by Ozonolysis of Different Double Bonds. *J. Phys. Chem. A* **2015**, *119*, 2318–2325.

- (9) Miliordos, E.; Xantheas, S. S. The Origin of the Reactivity of the Criegee Intermediate: Implications for Atmospheric Particle Growth. *Angew. Chem., Int. Ed.* **2016**, *55*, 1015–1019.
- (10) Bianchi, F.; Kurtén, T.; Riva, M.; Mohr, C.; Rissanen, M. P.; Roldin, P.; Berndt, T.; Crounse, J. D.; Wennberg, P. O.; Mentel, T. F.; Wildt, J.; Junninen, H.; Jokinen, T.; Kulmala, M.; Worsnop, D. R.; Thornton, J. A.; Donahue, N.; Kjaergaard, H. G.; Ehn, M. Highly Oxygenated Organic Molecules (HOM) from Gas-Phase Autoxidation Involving Peroxy Radicals: A Key Contributor to Atmospheric Aerosol. *Chem. Rev.* **2019**, *119*, 3472–3509.
- (11) Ehn, M.; Thornton, J. A.; Kleist, E.; Sipilä, M.; Junninen, H.; Pullinen, I.; Springer, M.; Rubach, F.; Tillmann, R.; Lee, B.; Lopez-Hilfiker, F.; Andres, S.; Acir, I. H.; Rissanen, M.; Jokinen, T.; Schobesberger, S.; Kangasluoma, J.; Kontkanen, J.; Nieminen, T.; Kurtén, T.; Nielsen, L. B.; Jørgensen, S.; Kjaergaard, H. G.; Canagaratna, M.; Maso, M. D.; Berndt, T.; Petäjä, T.; Wahner, A.; Kerminen, V.-M.; Kulmala, M.; Worsnop, D. R.; Wildt, J.; Mentel, T. F. A Large Source of Low-Volatility Secondary Organic Aerosol. *Nature* **2014**, *506*, 476–479.
- (12) Mentel, T. F.; Springer, M.; Ehn, M.; Kleist, E.; Pullinen, I.; Kurtén, T.; Rissanen, M.; Wahner, A.; Wildt, J. Formation of highly oxidized multifunctional compounds: autoxidation of peroxy radicals formed in the ozonolysis of alkenes - deduced from structure-product relationships. *Atmos. Chem. Phys.* **2015**, *15*, 6745–6765.
- (13) Mackenzie-Rae, F. A.; Liu, T.; Deng, W.; Saunders, S. M.; Fang, Z.; Zhang, Y.; Wang, X. Ozonolysis of α -phellandrene - Part I: Gas- and particle-phase characterisation. *Atmos. Chem. Phys.* **2017**, *17*, 6583–6609.
- (14) Zhao, Y.; Wingen, L. M.; Perraud, V.; Finlayson-Pitts, B. J. Phase, composition, and growth mechanism for secondary organic aerosol from the ozonolysis of α -cedrene. *Atmos. Chem. Phys.* **2016**, *16*, 3245–3264.
- (15) Ziemann, P. J. Formation of Alkoxyhydroperoxy Aldehydes and Cyclic Peroxyhemiacetals from Reactions of Cyclic Alkenes with O₃ in the Presence of Alcohols. *J. Phys. Chem. A* **2003**, *107*, 2048–2060.
- (16) Tong, H.; Lakey, P. S. J.; Arangio, A. M.; Socorro, J.; Shen, F.; Lucas, K.; Brune, W. H.; Pöschl, U.; Shiraiwa, M. Reactive Oxygen Species Formed by Secondary Organic Aerosols in Water and Surrogate Lung Fluid. *Environ. Sci. Technol.* **2018**, *52*, 11642–11651.
- (17) Campbell, S. J.; Stevanovic, S.; Miljevic, B.; Bottle, S. E.; Ristovski, Z.; Kalberer, M. Quantification of Particle-Bound Organic Radicals in Secondary Organic Aerosol. *Environ. Sci. Technol.* **2019**, *53*, 6729–6737.
- (18) Wang, M.; Yao, L.; Zheng, J.; Wang, X.; Chen, J.; Yang, X.; Worsnop, D. R.; Donahue, N. M.; Wang, L. Reactions of Atmospheric Particulate Stabilized Criegee Intermediates Lead to High-Molecular-Weight Aerosol Components. *Environ. Sci. Technol.* **2016**, *50*, 5702–5710.
- (19) Zhou, S.; Joudan, S.; Forbes, M. W.; Zhou, Z.; Abbatt, J. P. D. Reaction of Condensed-Phase Criegee Intermediates with Carboxylic Acids and Perfluoroalkyl Carboxylic Acids. *Environ. Sci. Technol. Lett.* **2019**, *6*, 243–250.
- (20) Mochida, M.; Katrib, Y.; Jayne, J. T.; Worsnop, D. R.; Martin, S. T. M. The Relative Importance of Competing Pathways for the Formation of High-Molecular-Weight Peroxides in the Ozonolysis of Organic Aerosol Particles. *Atmos. Chem. Phys.* **2006**, *6*, 4851–4866.
- (21) Zhou, Z.; Abbatt, J. P. D. Formation of Gas-Phase Hydrogen Peroxide via Multiphase Ozonolysis of Unsaturated Lipids. *Environ. Sci. Technol. Lett.* **2021**, *8*, 114–120.
- (22) Coffaro, B.; Weisel, C. P. Reactions and Products of Squalene and Ozone: A Review. *Environ. Sci. Technol.* **2022**, *56*, 7396–7411.
- (23) Arata, C.; Heine, N.; Wang, N.; Misztal, P. K.; Wargocki, P.; Bekö, G.; Williams, J.; Nazaroff, W. W.; Wilson, K. R.; Goldstein, A. H. Heterogeneous Ozonolysis of Squalene: Gas-Phase Products Depend on Water Vapor Concentration. *Environ. Sci. Technol.* **2019**, *53*, 14441–14448.
- (24) Giorio, C.; Campbell, S. J.; Bruschi, M.; Tampieri, F.; Barbon, A.; Toffoletti, A.; Tapparo, A.; Paijens, C.; Wedlake, A. J.; Grice, P.; Howe, D. J.; Kalberer, M. Online Quantification of Criegee Intermediates of α -Pinene Ozonolysis by Stabilization with Spin Traps and Proton-Transfer Reaction Mass Spectrometry Detection. *J. Am. Chem. Soc.* **2017**, *139*, 3999–4008.
- (25) Giorio, C.; Campbell, S. J.; Bruschi, M.; Archibald, A. T.; Kalberer, M. Detection and Identification of Criegee Intermediates from the Ozonolysis of Biogenic and Anthropogenic VOCs: Comparison between Experimental Measurements and Theoretical Calculations. *Faraday Discuss.* **2017**, *200*, 559–578.
- (26) Welz, O.; Savee, J. D.; Osborn, D. L.; Vasu, S. S.; Percival, C. J.; Shallcross, D. E.; Taatjes, C. Direct Kinetic Measurements of Criegee Intermediate (CH₂OO) Formed by Reaction of CH₂I with O₂. *Science* **2012**, *335*, 204–207.
- (27) Taatjes, C. A.; Welz, O.; Eskola, A. J.; Savee, J. D.; Scheer, A. M.; Shallcross, D. E.; Rotavera, B.; Lee, E. P. F.; Dyke, J. M.; Mok, D. K. W.; Osborn, D. L.; Percival, C. J. Direct Measurements of Conformer-Dependent Reactivity of the Criegee Intermediate CH₃CHOO. *Science* **2013**, *340*, 177–180.
- (28) Yu, K. P.; Chen, Y. P.; Gong, J. Y.; Chen, Y. C.; Cheng, C. C. Improving the Collection Efficiency of the Liquid Impinger for Ultrafine Particles and Viral Aerosols by Applying Granular Bed Filtration. *J. Aerosol Sci.* **2016**, *101*, 133–143.
- (29) Jenkin, M. E.; Wyche, K. P.; Evans, C. J.; Carr, T.; Monks, P. S.; Alfarra, M. R.; Barley, M. H.; McFiggans, G. B.; Young, J. C.; Rickard, A. R. Development and chamber evaluation of the MCM v3.2 degradation scheme for β -caryophyllene. *Atmos. Chem. Phys.* **2012**, *12*, 5275–5308.
- (30) Vereecken, L.; Novelli, A.; Taraborrelli, D. Unimolecular Decay Strongly Limits the Atmospheric Impact of Criegee Intermediates. *Phys. Chem. Chem. Phys.* **2017**, *19*, 31599–31612.
- (31) Winterhalter, R.; Herrmann, F.; Kanawati, B.; Nguyen, T. L.; Peeters, J.; Vereecken, L.; Moortgat, G. K. The gas-phase ozonolysis of β -caryophyllene (C₁₅H₂₄). Part I: an experimental study. *Phys. Chem. Chem. Phys.* **2009**, *11*, 4152.
- (32) Nguyen, T. L.; Winterhalter, R.; Moortgat, G.; Kanawati, B.; Peeters, J.; Vereecken, L. The gas-phase ozonolysis of β -caryophyllene (C₁₅H₂₄). Part II: A theoretical study. *Phys. Chem. Chem. Phys.* **2009**, *11*, 4173–4183.
- (33) Vereecken, L.; Harder, H.; Novelli, A. The Reactions of Criegee Intermediates with Alkenes, Ozone, and Carbonyl Oxides. *Phys. Chem. Chem. Phys.* **2014**, *16*, 4039–4049.
- (34) Gallimore, P. J.; Griffiths, P. T.; Pope, F. D.; Reid, J. P.; Kalberer, M. Comprehensive Modeling Study of Ozonolysis of Oleic Acid Aerosol Based on Real-Time, Online Measurements of Aerosol Composition. *J. Geophys. Res.: Atmos.* **2017**, *122*, 4364–4377.
- (35) Maclean, A. M.; Smith, Y. R.; Li, Y.; Huang, Y.; Hettiyadura, A. P. S.; Crescenzo, G. V.; Shiraiwa, M.; Laskin, A.; Nizkorodov, S. A.; Bertram, A. K. Humidity-Dependent Viscosity of Secondary Organic Aerosol from Ozonolysis of β -Caryophyllene: Measurements, Predictions, and Implications. *ACS Earth Space Chem.* **2021**, *5*, 305–318.
- (36) Julin, J.; Winkler, P. M.; Donahue, N. M.; Wagner, P. E.; Riipinen, I. Near-Unity Mass Accommodation Coefficient of Organic Molecules of Varying Structure. *Environ. Sci. Technol.* **2014**, *48*, 12083–12089.
- (37) Zeng, M.; Wilson, K. R. Efficient Coupling of Reaction Pathways of Criegee Intermediates and Free Radicals in the Heterogeneous Ozonolysis of Alkenes. *J. Phys. Chem. Lett.* **2020**, *11*, 6580–6585.
- (38) Zaytsev, A.; Breitenlechner, M.; Novelli, A.; Fuchs, H.; Knopf, D.; Kroll, J.; Keutsch, F. Application of Chemical Derivatization Techniques Combined with Chemical Ionization Mass Spectrometry to Detect Stabilized Criegee Intermediates and Peroxy Radicals in the Gas Phase. *Atmos. Meas. Tech.* **2020**, *14*, 2501–2513.
- (39) Tong, H.; Zhang, Y.; Filippi, A.; Wang, T.; Li, C.; Liu, F.; Leppla, D.; Kourtchev, I.; Wang, K.; Keskinen, H. M.; Levula, J. T.; Arangio, A. M.; Shen, F.; Ditas, F.; Martin, S. T.; Artaxo, P.; Godoi, R. H. M.; Yamamoto, C. I.; de Souza, R. A. F.; Huang, R. J.; Berkemeier, T.; Wang, Y.; Su, H.; Cheng, Y.; Pope, F. D.; Fu, P.; Yao, M.; Pöhlker, C.; Petäjä, T.; Kulmala, M.; Andreae, M. O.; Shiraiwa, M.; Pöschl, U.

Hoffmann, T.; Kalberer, M. Radical Formation by Fine Particulate Matter Associated with Highly Oxygenated Molecules. *Environ. Sci. Technol.* **2019**, *53*, 12506–12518.